Wavelets for SAR Speckle Noise Filtering

Jaan-Rong Tsay [1*]

[1] Associate Prof. Dr.-Ing., Department of Geomatics, National Cheng Kung University(NCKU), No.1, University Road, Tainan City 701, Taiwan (R.O.C.)

*tsayjr@mail.ncku.edu.tw

***Abstract*:** *The well-known filters for reducing SAR speckle noises are reviewed. The reason causing the cross-like pattern which often appears in the SAR images after speckle filtering e.g. by using the Goldstein filter is given and analyzed. To reduce SAR speckle noises properly and reserve SAR image features with better performance, this paper presents an algorithm developed at NCKU for filtering Synthetic Aperture Radar (SAR) speckle-noise based on wavelets. Orthogonal wavelets, e.g. Haar wavelets, asymmetric Daubechies (AD) wavelets, and least asymmetric Daubechies (LAD) wavelets, are used to perform 2D FWT(=Fast Wavelet Transform) for SAR images. The determined wavelet coefficients are then utilized to reduce SAR speckle noise. It combines the soft thresholding method and multi-resolution analysis (MRA) using orthogonal wavelets. The computation program is developed in FORTRAN. Test results show that cross-like pattern don't appear anymore. Haar wavelets perform a better edge preservation ability with a larger ρ-values ranging from 0.0532 to 1.0000, but worse noise filtering ability with S/M-values ranging from 0.0332 to 0.2545, where the original image has the S/M-value of 0.2507. Compared to Haar wavelets, both LAD and AD wavelets perform a better speckle filtering but a worse edge preservation effect.*

Keywords: Synthetic Aperture Radar(SAR), speckle, noise, filtering, 2D discrete wavelet transform(DWT)

Introduction

As we know, terrain surfaces cannot be imaged clearly with visible or infrared sensors in improper weather due to clouds, fog, dust, or smoke in the atmosphere. Especially in Taiwan, only about 60 days are suitable each year for taking clear aerial images. Microwaves can penetrate through clouds, fog, vegetation canopy, and soil on terrain surfaces. Also, they can operate day and night. Therefore, spaceborne or airborne Synthetic Aperture Radar (SAR) might provide a state-of-the-art and applicable technology and a good solution for acquiring high-resolution spatial data and information on the terrain surface in Taiwan, especially in some emergent areas damaged e.g. by typhoons, earthquakes, heavy rainfall, or landslide, when clear aerial images cannot be taken due to bad weather and atmospheric conditions.

Backscattering value of a pixel in SAR image is a coherent sum of all contributions of the scatterers in the corresponding resolution cell. Constructive or destructive contributions might appear in neighboring pixels so that an inherently exist salt-pepper noise called

'speckle' appears in SAR images. Speckle degrades the SAR image quality and makes interpretation of SAR image features more difficult because the "salt and pepper" effect corrupts information about the surface. Therefore, speckle must be reduced, or even ideally removed completely, somehow.

Literature Review

Speckle may be reduced according to different criterions with minimum loss of radiometric, edge, textural information or spatial resolution. Briefly to say, diverse kinds of speckle filters can be divided into mono- and multi-temporal ones. Mono-temporal filters also can be classified according to spatial domain or frequency domain. Spatial domain filters include adaptive or non-adaptive filters. For example, mean or median filters are non-adaptive ones. Examples of adaptive filters are Lee filters, refined Lee filters, Kuan filter, Gamma Map filters, Frost filters. On the other hand, multi-looking belongs to speckle reduction defined in frequency domain. Multi-temporal filters include e.g. the texture compensation multichannel fliter, 3D adaptive neighborhood filter, and time-space filter [1].

Formation of SAR Speckle Noise

Full-resolution SAR imagery has a grainy appearance called speckle, which is a phenomenon due to the coherent nature of SAR imaging. The number and arrangement of scattering elements within one resolution cell varies from pixel to pixel. Returned signal *s* is a coherent combination of the returns from the scattering elements within the resolution cell, and can be represented as follows [2].

$$s = \mathrm{A} e^{-\frac{4\pi i}{\lambda}\rho} \sum_{k=1}^{N} a_k \, e^{-\frac{4\pi i}{\lambda}\Delta\rho_k} \quad (1)$$

where

$e^{-\frac{4\pi i}{\lambda}\rho}$ denotes the range phase,

$\sum_{k=1}^{N} a_k \, e^{-\frac{4\pi i}{\lambda}\Delta\rho_k}$ expresses the scatterer contribution.

The slight difference in distance means that the returning waves from within a single pixel may be in phase or out of phase by varying degrees when received by the sensor. Where the returning waves are in phase with one another, the intensity of the resulting combined signal will be amplified by constructive interference. At the opposite extreme, where returning waves from within a single pixel are at completely opposite phases (that is, when one wave is at the peak of its cycle and another is at the trough), they will tend to cancel each other

out, reducing the intensity of the combined signal (this is known as destructive interference). Constructive and destructive interference produces a seemingly random pattern of brighter and darker pixels in radar images, giving them the distinctly graining appearance known as speckle. Because of the effect of speckle, the resulting radar image will show pseudo-random variations in the apparent backscatter from every pixel in the image. This makes it more difficult to identify and differentiate features within the imagery. Speckle is often described imprecisely as “random noise”, but it is important to realize that the seemingly random variations in backscatter are a direct result of the subpixel-scale geometry of the radar illumination conditions. Thus, if two images are acquired from the same position, with the same wavelength and polarization, and with the same ground surface conditions, the speckle pattern in the two images will be highly correlated. In fact, this principle is employed as part of the process of radar interferometry [3].

Briefly to say, speckle is a granular noise that inherently exists in and degrades the quality of SAR images.

Cross-like Pattern and Goldstein Filter

Speckle can be reduced through the application of image processing techniques, such as averaging neighboring pixel values, or by special filtering and averaging techniques such as the Goldstein filter, but cannot be completely eliminated. SNAP (=Sentinel Application Platform) software system utilizes the Goldstein filter [4] to reduce the speckle noise. In that filtering process, 2D FFT (=Fast discrete Fourier Transform) is used. The principal advantage of the separability property of 2D FFT is that F(u,v) or f(x,y) can be obtained in two steps by successive application of the 1D Fourier transform or its inverse. All values of f(x) contribute to each of the terms of the DFT. Many high buildings exist in urban areas so that the backscattered energy of microwaves is strong due to the double-bounce mechanism. It forms significantly bright pixels in the SAR images with high power. Therefore, cross-like patterns appear in the phase data filtered by using the Goldstein filter as shown in Figure 1.

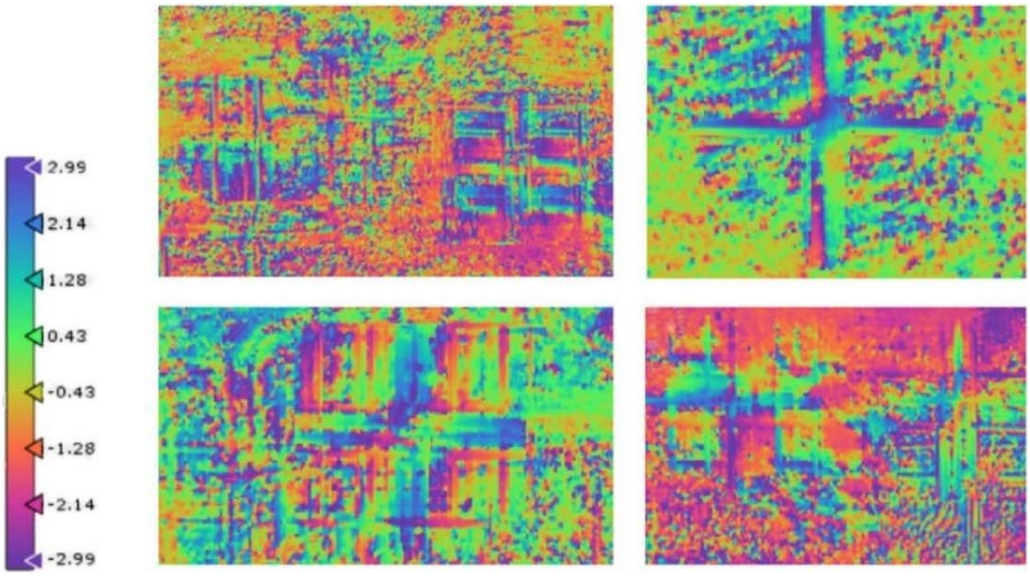

Figure 1: Example of cross-like patterns in the filtered phase data by Goldstein filter [5].

Wavelets for SAR Speckle Filtering

To avoid the above-mentioned effect of cross-like patterns, an autonomous research and development is thus motivated. In this paper, the SAR image speckle is reduced as follows. Firstly, the equations for 1D image decomposition [6] are conducted for each row and column vector, respectively:

$$S_k = \sum_{m=0}^{2N-1} h_m \cdot G_{2k+m-1} \quad (2)$$

$$D_k = \sum_{m=0}^{2N-1} (-1)^m h_{(2N-1)-m} \cdot G_{2k+m-1} \quad (3)$$

where $\{S_k, D_k, \forall k\}$ are the approximation and detail components of the input pixel values $\{G_n \forall n\}$; $\{h_m, \forall k\}$ are the known low-pass filter coefficients. In this paper, all tests are done using the Haar wavelets, the asymmetric Daubechies wavelets, and the least asymmetric Daubechies wavelets.

The low-pass filter coefficients h_n, n=0 (1) 1, for the Haar wavelets are:

$$h_0 = \frac{1}{\sqrt{2}} \qquad h_1 = \frac{1}{\sqrt{2}}$$

Daubechies father wavelet $\phi(x)$ can not be expressed in explicit form, but it can be computed somehow, e.g. by means of sub-division algorithm, Strang's method, Fourier algorithm, or Kaiser's method of cumulants. The low-pass filter coefficients h_n, n=0 (1) 7, for the compactly supported asymmetric wavelets of Daubechies of order 4 (N=4) are [7]:

h_0 = +0.2303778133088964 h_1 = 0.7148465705529154 h_2 = 0.6308807679398587
h_3 = –0.0279837694168599 h_4 = – 0.1870348117190931 h_5 = 0.0308413818355607
h_6 = +0.0328830116668852 h_7 = –0.0105974017850690

with $\sum_{n=0}^{7} h_n = \sqrt{2}$.

The low-pass filter coefficients h_n, n=0 (1) 7, for the compactly supported least-asymmetric wavelets of Daubechies of order 4 (N=4) are [7]:

h_0 = +0.045570345896 h_1 = –0.017824701442 h_2 = –0.140317624179
h_3 = +0.421234534204 h_4 = +1.136658243408 h_5 = +0.703739068656
h_6 = –0.041910965125 h_7 = –0.107148901418

with $\sum_{n=0}^{7} h_n = 2$. They must be multiplied with a constant $1/\sqrt{2}$ so that $\sum_{n=0}^{7} h_n = \sqrt{2}$.

The multi-resolution analysis (MRA) is performed using orthogonal wavelet decomposition. Therefore, the approximations $\{S_k, \forall k\}$ are then decomposed to obtain the approximation and detail components on a coarser resolution level. This process is conducted level by level as illustrated by Figure 2 from left to right.
Then, the average $\bar{d}$ and standard deviation $\hat{\sigma}_d$ of all detail components $\{D_k, \forall k\}$ on all levels are calculated. The soft thresholding process is then performed for all detail components $\{D_k, \forall k\}$ as follows [8]:

$$D_i = \begin{cases} D_i - \varepsilon & if\ D_i > \varepsilon \\ 0 & if\ -\varepsilon \le D_i \le \varepsilon \\ D_i + \varepsilon & if\ D_i < -\varepsilon \end{cases} \quad (4)$$

where

a threshold $\varepsilon = t \cdot \hat{\sigma}_d$ is used,
t is an input multiplication constant, e.g. t=1.50.

After soft thresholding is completed, multi-resolution reconstruction is conducted as shown in Figure 2 from right to left. The equation for 1D image reconstruction [6] is conducted for each column and row vector, respectively:

$$G_n = \sum_m \{h_m \cdot S_k + (-1)^m h_{(2N-1)-m} \cdot D_k\} \quad (5)$$

where

$m = n - 2k + 1$;
m = 0 (2) $2N$-2 for n = odd number;
m = 1 (2) $2N$-1 for n = even number.

Figure 2 illustrates an example of consecutive multi-resolution image decomposition and image reconstruction with four resolution levels [9].

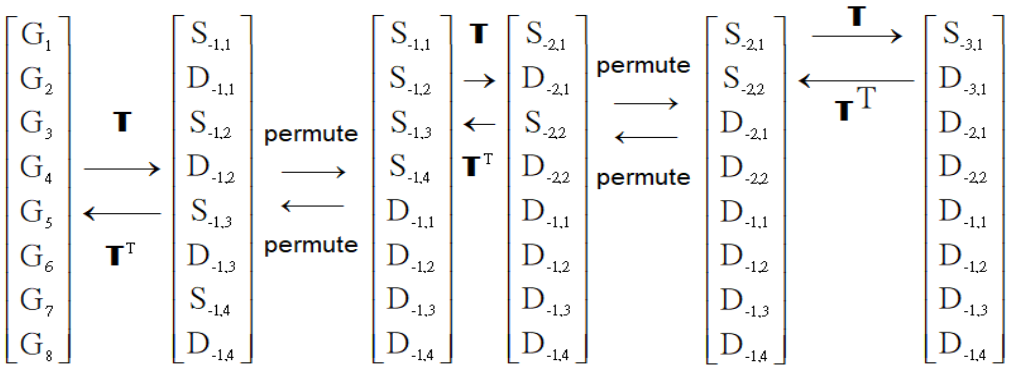

Figure 2: Multi-resolution image decomposition and reconstruction [9].

The multi-resolution image reconstruction is performed from coarse to fine level. It is well-known that a 2D multi-resolution decomposition and reconstruction can be conducted by two 1D image decomposition and reconstruction e.g. along each column first and then along each row, in the case of orthogonal wavelet decomposition and reconstruction. After the processes mentioned above are completed, the denoised image is obtained.
For quantitative evaluation, an extensively used measure is the root mean square error (RMSE) defined as

$$\mathrm{RMSE} = \sqrt{\frac{1}{K}\sum_{i=1}^{K}\left(G_i - \hat{G}_i\right)^2} \tag{6}$$

where G is the original image, $\hat{G}$ is the denoised image, and K is the image size. Also, in order to quantify the speckle reduction performance, one can compute the standard-deviation-to-mean ratio (S/M). That is a measure of image speckle in homogeneous areas. Moreover, a qualitative measure ρ is used for expressing edge preservation performance originally defined in [10]:

$$\rho = \frac{\Gamma\left(\Delta G - \overline{\Delta G}, \Delta\hat{G} - \overline{\Delta\hat{G}}\right)}{\sqrt{\Gamma\left(\Delta G - \overline{\Delta G}, \Delta G - \overline{\Delta G}\right)\cdot\Gamma\left(\Delta\hat{G} - \overline{\Delta\hat{G}}, \Delta\hat{G} - \overline{\Delta\hat{G}}\right)}} \tag{7}$$

where ΔG and $\Delta\hat{G}$ are the high-pass filtered version of G and $\hat{G}$, respectively, obtained with a 3 x 3-pixel standard approximation of the Laplacian operator F [11],

$$\mathrm{F} = \begin{bmatrix} 0 & -1 & 0 \\ -1 & 4 & -1 \\ 0 & -1 & 0 \end{bmatrix} \tag{8}$$

the overline operator represents the mean value, and

$$\Gamma(G^1, G^2) = \sum_{i=1}^{K} G_i^1 \cdot G_i^2 \tag{9}$$

The correlation measure, ρ should be close to unity for an optimal effect of edge preservation [12].

Tests and Analysis

The computation program for the SAR speckle reduction using the data processing steps mentioned above is developed in FORTRAN. Tests are done using the SAR image of 512 x 512 pixels extracted from [13]. Figure 3 shows that it is full of speckles. The input noisy image in Figure 3 has the minimal and maximal gray values of 0 and 255, respectively. The number L of levels used in all tests includes 1,2,3,4 or 5. Soft thresholding adopts different thresholds $\varepsilon = t \cdot \hat{\sigma}_d$ with t=0.0, 0.5, 1.0, 1.5, 2.0 and 3.0. Three kinds of orthogonal wavelets are used. They are Haar wavelets, least-asymmetric Daubechies wavelets, and asymmetric Daubechies wavelets. Altogether 3 x 5 x 6 = 90 tests are done.

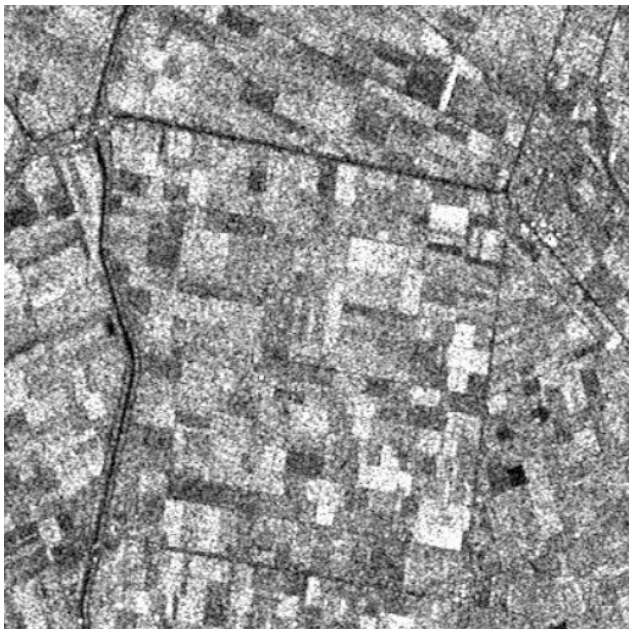

Figure 3: Test image of 512 x 512 pixels from [13]

Figure 4 illustrates a denoised image using Haar wavelets with L=3 and t=1.5. Apparently, cross-like patterns caused by the Goldstein filter do not appear anymore in the denoised image by the method combining the multi-resolution orthogonal wavelet decomposition and reconstruction as well as the soft thresholding scheme. Table 1 shows the parameter values. The gray values of the denoised image are changed from the range [0, 255] of the original input noisy image to $[g_0, g_1]$, where g_0 and g_1 denote the minimal and maximal gray values of the denoised image, respectively. Table 1 illustrates that some cases have $g_1>255$. To generate its denoised image, the gray values of the output denoised image are linearly transformed to the range [0, 255]. On the other hand, Table 1 shows that the values of the correlation measure ρ range from 0.0532 to 1.0000. As stated above, the correlation measure ρ should be close to unity for an optimal effect of edge preservation. Therefore, Table 1 illustrates clearly that Haar wavelets perform a better edge preservation ability with a larger ρ-values ranging from 0.0532 to 1.0000. Moreover, the standard-deviation-to-mean ratios (S/M) range from 0.0332 to 0.2545, where the original image has the S/M-value of 0.2507. It demonstrates that image noise is reduced apparently. Furthermore, the RMSE-values are increased for larger t-values of the soft thresholding. That means more noises are removed if a larger threshold ε is adopted. Also, One can observe that the larger the ρ-values, the smaller the RMSE-values and the larger the S/M-values. That means that one gets a better edge preservation at the expense of a worse noise-filtering effect.

Figure 5 shows the denoised images with L=3 and t=0.0 to t=3.0. It demonstrates that larger thresholds provide a better smoothing effect, but a worse edge preservation ability. Figure 6 shows the denoised images with t=2.0 and L=1 to L=5. Figure 6 and Table 1 tell us that a larger number of levels gives a better noise-filtering effect at the expense of worse edge preservation effect.

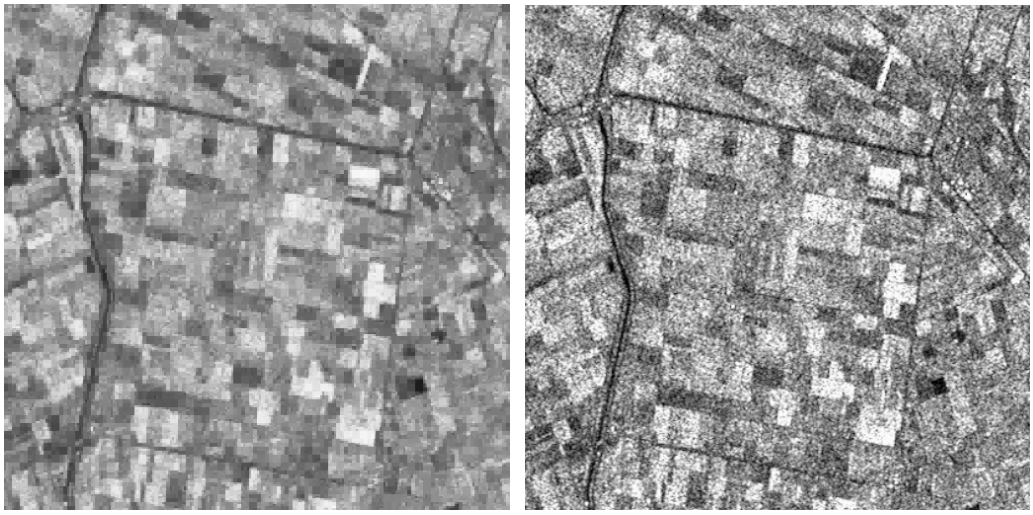

Figure 4: Denoised image (left: HAAR, L=3, t=1.5) and its original SAR image(right)

Table 1: Parameter values determined by the denoising method using Haar wavelets

	L=1, d_i = 0.0 ± 23.8					L=2, d_i = -0.0 ± 33.0				
t	g_0	g_1	ρ	S/M	RMSE	g_0	g_1	ρ	S/M	RMSE
0.0	0	255	1.0000	0.2518	0.00	0	255	1.0000	0.2518	0.00
0.5	1	253	0.8715	0.1582	8.38	4	255	0.7973	0.1216	12.52
1.0	1	253	0.6822	0.1440	13.59	6	256	0.5331	0.1120	20.12
1.5	1	253	0.5438	0.1362	16.75	6	257	0.3469	0.1005	24.64
2.0	1	253	0.4589	0.1330	18.58	6	253	0.2330	0.0869	27.06
3.0	1	253	0.3858	0.1320	20.10	6	250	0.1296	0.0820	29.88
	L=3, d_i = -0.0 ± 39.7					L=4, d_i = -0.1 ± 45.1				
t	g_0	g_1	ρ	S/M	RMSE	g_0	g_1	ρ	S/M	RMSE
0.0	0	255	1.0000	0.2545	0.00	0	255	1.0000	0.2545	0.00
0.5	8	253	0.7522	0.1087	14.90	13	251	0.7124	0.1003	16.49
1.0	11	251	0.4735	0.0808	23.24	20	249	0.4232	0.0739	25.24
1.5	13	248	0.2909	0.0666	28.18	24	243	0.2503	0.0592	30.32
2.0	14	246	0.1811	0.0570	31.31	25	242	0.1517	0.0492	33.60
3.0	14	245	0.0781	0.0463	34.92	31	242	0.0625	0.0369	37.56
	L=5, d_i = -0.1 ± 49.5									
t	g_0	g_1	ρ	S/M	RMSE					
0.0	0	255	1.0000	0.2545	0.00					
0.5	14	250	0.6791	0.0948	17.65					
1.0	23	244	0.3834	0.0693	26.58					
1.5	31	240	0.2188	0.0550	31.66					
2.0	36	239	0.1304	0.0451	34.95					
3.0	40	236	0.0532	0.0332	39.00					

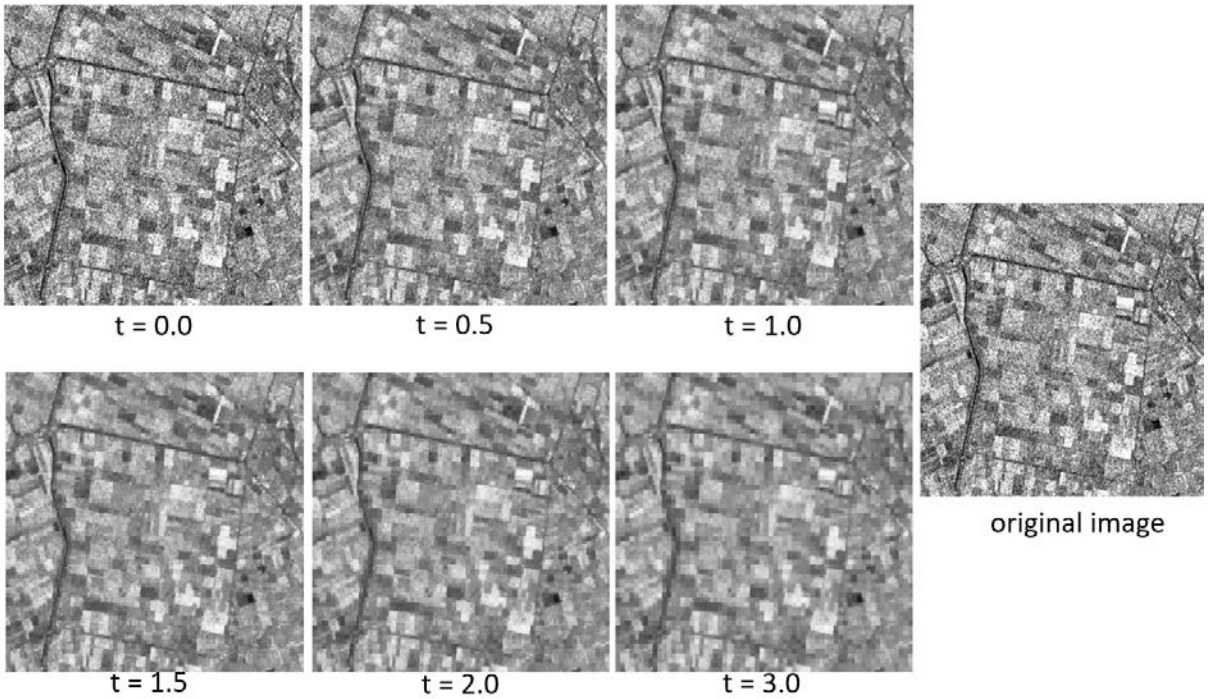

Figure 5: Soft Thresholding, L=3, Haar Wavelets

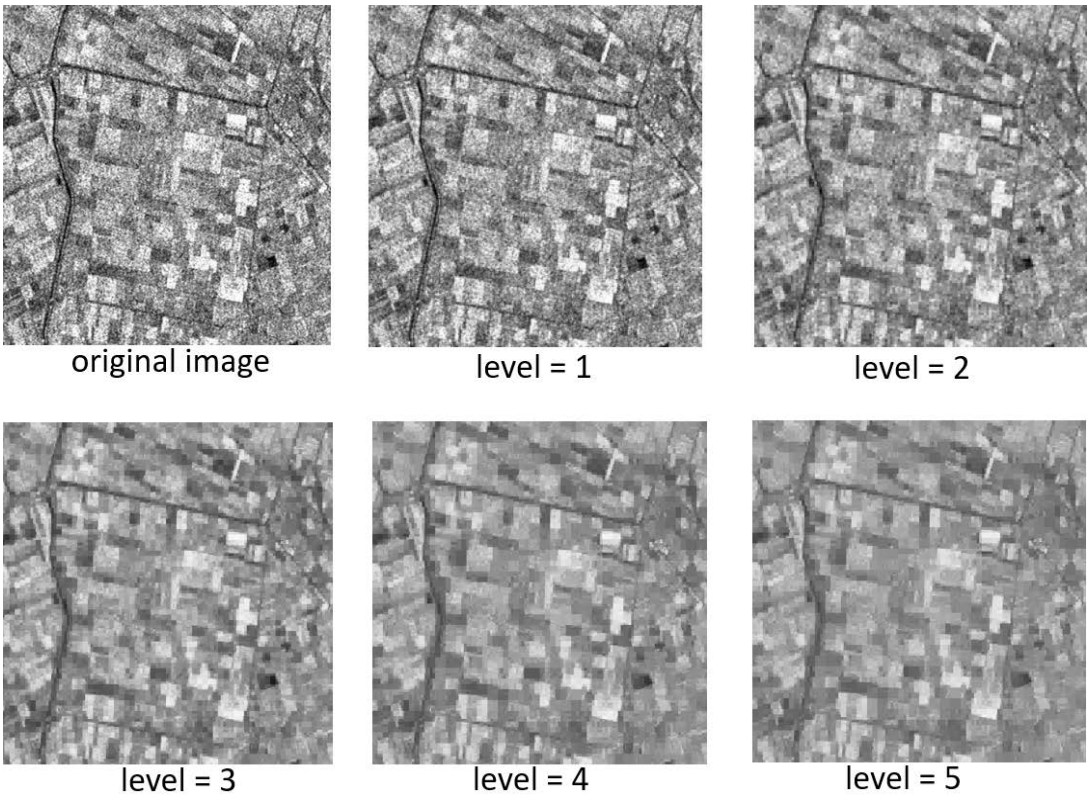

Figure 6: Soft Thresholding, Haar Wavelets, t=2.0

Figure 7 shows a denoised image using the least-asymmetric Daubechies (LAD) wavelets with L=3 and t=1.5. No cross-like patterns appear, too. Also, the speckle is reduced. Table 2 illustrates the parameter values. The asymmetry property of Daubechies wavelets causes the image translation effect. Although it does not influence image feature interpretation at all,

accurate georeferencing must be conducted using additional amendments. Table 1 shows that the ρ-values range from -0.0051 to 0.0023, and the S/M-values range from 0.0410 to 0.1259. Comparing with the Haar wavelets, the least-asymmetric Daubechies wavelets perform a worse edge preservation ability with the ρ-values ranging from -0.0051 to 0.0023, but a better performance of speckle filtering with the S/M-values ranging from 0.0410 to 0.1259, where the original image has the S/M-value of 0.2507. Almost all denoised images have the gray values with $g_0<0$ or $g_1>255$. Therefore, they are transformed linearly from $[g_0, g_1]$ to [0, 255] or $[g_{min}, g_{max}]$, where g_{min} and g_{max} denote the minimal and maximal gray value of the input image, respectively. Moreover, the image translation effect caused by the asymmetric property of Daubechies must be studied further for georeferencing applications, especially in Taiwan. Figure 8 illustrates the denoised images with L=3 and t=0.0 to t=3.0. Also, Figure 9 shows the denoised images with t=2.0 and L=1 to L=5. Similar to Haar wavelets, LAD wavelets give a better smoothing effect, but a worse performance on edge preservation, if a larger threshold is applied. Also, a larger number of levels gives a better noise-filtering effect at the expense of worse edge preservation effect.

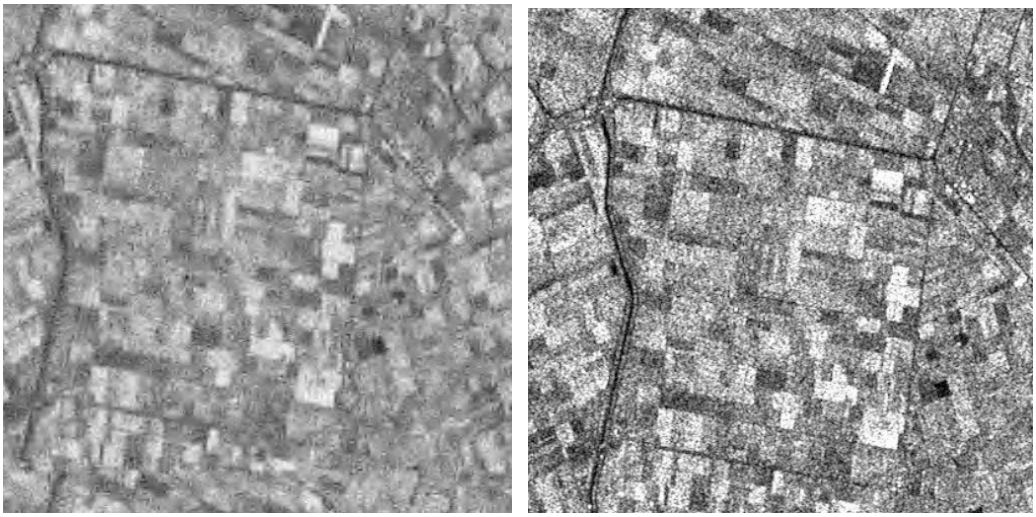

Figure 7: Denoised image (left: LAD, L=3, t=1.5) and its original SAR image(right)

Table 2: Parameter values determined by the denoising method using least asymmetric Daubechies wavelets (N=4)

	L=1, d_i = 0.0 ± 18.3					L=2, d_i = 0.0 ± 30.1				
t	g_0	g_1	ρ	S/M	RMSE	g_0	g_1	ρ	S/M	RMSE
0.0	0	255	-0.0051	0.2507	0.00	-56	322	-0.0018	0.1022	25.23
0.5	-8	265	-0.0051	0.1259	7.51	-42	311	-0.0009	0.0859	23.71
1.0	-14	276	-0.0049	0.1118	12.40	-29	296	-0.0002	0.0811	23.29
1.5	-15	284	-0.0047	0.1100	15.52	-19	292	0.0004	0.0801	24.75
2.0	-16	291	-0.0043	0.1080	17.82	-17	288	0.0009	0.0758	25.98
3.0	-16	299	-0.0038	0.1097	20.42	-19	293	-0.0002	0.0708	28.78
	L=3, d_i = -0.0 ± 37.4					L=4, d_i = 0.0 ± 43.4				
t	g_0	g_1	ρ	S/M	RMSE	g_0	g_1	ρ	S/M	RMSE
0.0	-34	286	0.0015	0.0571	33.71	-90	353	-0.0013	0.0653	52.03
0.5	-49	306	0.0007	0.0603	34.62	-62	321	-0.0000	0.0598	50.64
1.0	-61	328	-0.0002	0.0659	36.00	-47	299	0.0011	0.0557	49.77
1.5	-85	355	-0.0013	0.0740	38.51	-37	289	0.0020	0.0527	48.92

2.0	-18	277	0.0014	0.0603	33.18	-25	284	0.0008	0.0514	48.25
3.0	-18	277	0.0000	0.0521	34.25	-19	281	0.0006	0.0461	47.40

	L=5, d_i = 0.1 ± 48.7				
t	g_0	g_1	ρ	S/M	RMSE
0.0	-101	361	-0.0012	0.0637	59.39
0.5	-74	326	0.0002	0.0574	58.98
1.0	-57	302	0.0016	0.0524	58.90
1.5	-45	286	0.0020	0.0487	58.83
2.0	-37	275	0.0010	0.0453	58.74
3.0	-22	268	0.0023	0.0410	57.78

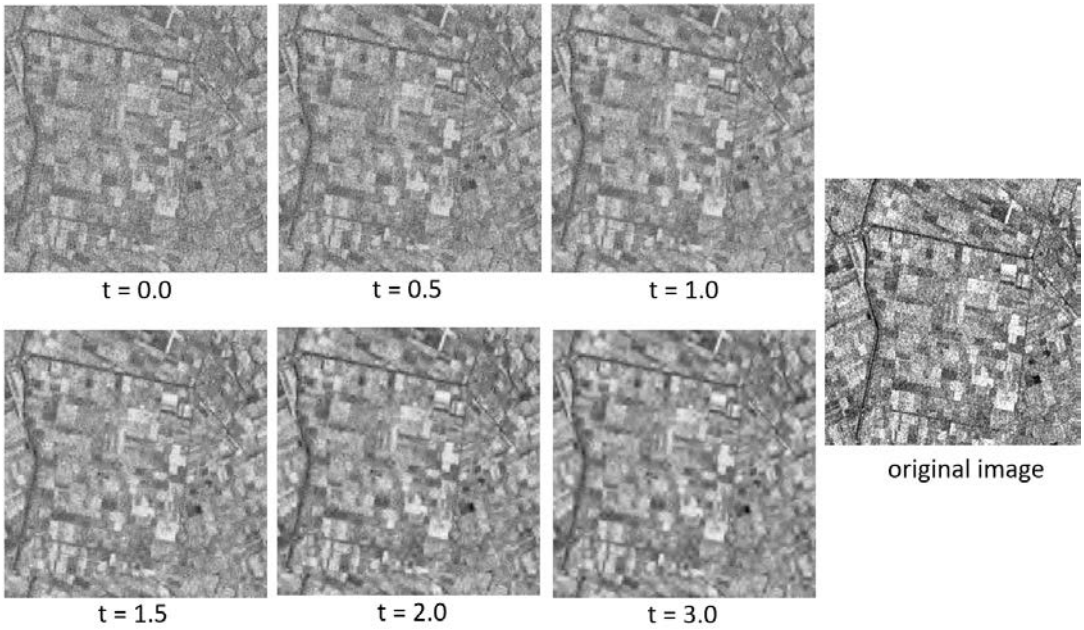

Figure 8: Soft Thresholding, L=3, L.A. Daub. Wavelets (N=4)

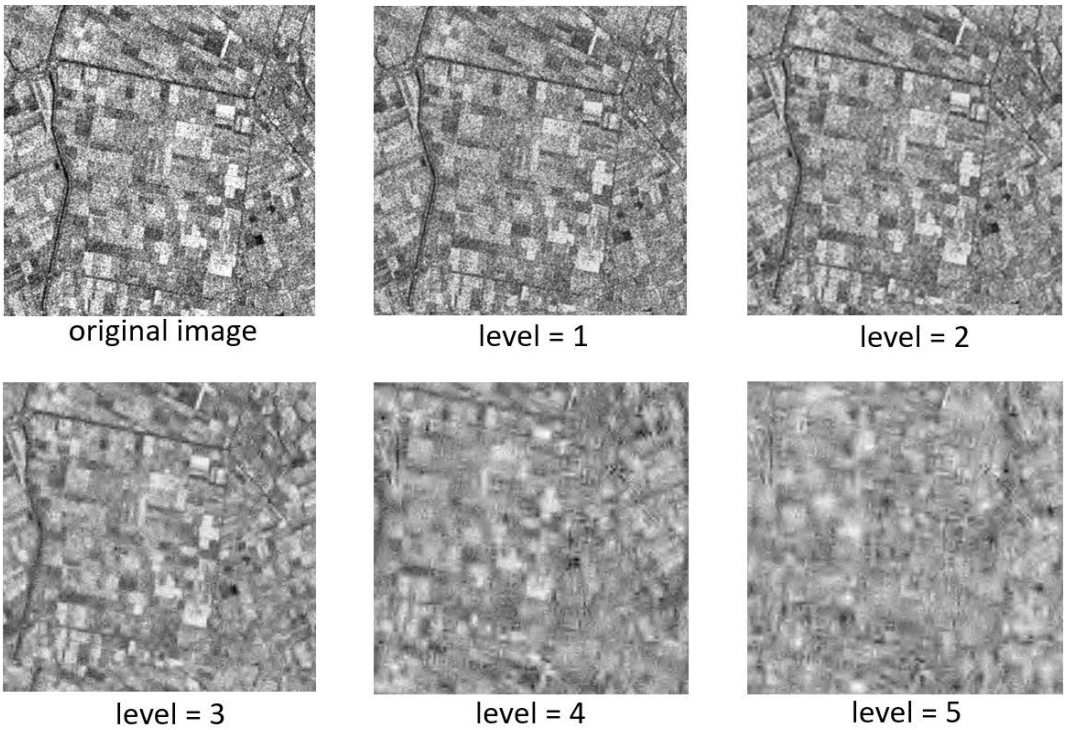

Figure 9: Soft Thresholding, L.A. Daub. Wavelets (N=4), t=2.0

Figure 10 shows the denoised image using the asymmetric Daubechies wavelets with L=3 and t=1.5. Apparently, no cross-like patterns appear, either. Table 3 illustrates the parameter values, where the asymmetric Daubechies wavelets perform a worse edge preservation ability with the ρ-values ranging from -0.0059 to 0.0025, but a better performance of speckle filtering with the S/M-values ranging from 0.0450 to 0.1356, where the original image has the S/M-value of 0.2507. Figure 11 shows the denoised images with L=3 and t-0.0 to t=3.0, and Figure 12 demonstrates the denoised images with t=2.0 and L=1 to L=5. Similar to both Haar and LAD wavelets, AD wavelets give a better smoothing effect, but a worse performance on edge preservation, if a larger threshold is applied. Also, a larger number of levels gives a better noise-filtering effect at the expense of worse edge preservation.

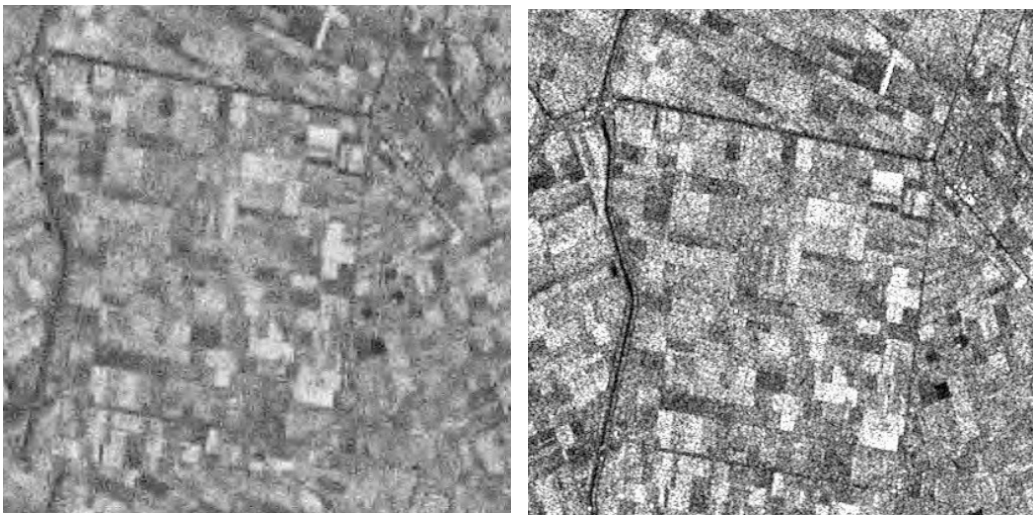

Figure 10: Denoised image (left: AD, L=3, t=1.5) and its original SAR image(right)

Table 3: Parameter values determined by the denoising method using asymmetric Daubechies wavelets (N=4)

	L=1, d_i = 0.0 ± 18.3					L=2, d_i = -0.0 ± 30.1				
t	g_0	g_1	ρ	S/M	RMSE	g_0	g_1	ρ	S/M	RMSE
0.0	0	255	-0.0051	0.2507	0.00	-50	318	-0.0059	0.1048	24.80
0.5	-7	267	-0.0042	0.1356	7.79	-37	304	-0.0053	0.0909	22.99
1.0	-8	275	-0.0024	0.1287	12.47	-26	287	-0.0038	0.0842	22.48
1.5	-11	277	-0.0010	0.1189	14.50	-18	275	-0.0030	0.0806	23.24
2.0	-14	279	-0.0001	0.1111	15.83	-9	277	-0.0020	0.0825	25.17
3.0	-19	281	0.0012	0.1035	17.12	-13	282	-0.0016	0.0740	28.00
	L=3, d_i = -0.0 ± 37.4					L=4, d_i = 0.0 ± 43.2				
t	g_0	g_1	ρ	S/M	RMSE	g_0	g_1	ρ	S/M	RMSE
0.0	-78	339	-0.0051	0.0712	38.30	-89	372	-0.0051	0.0689	51.80
0.5	-42	325	-0.0038	0.0745	36.17	-58	331	-0.0034	0.0644	50.53
1.0	-33	313	-0.0025	0.0692	34.95	-45	317	-0.0020	0.0608	49.42
1.5	-27	301	-0.0010	0.0643	34.19	-40	309	-0.0005	0.0565	48.52
2.0	-21	290	-0.0001	0.0603	33.88	-33	298	0.0001	0.0527	47.97
3.0	-7	279	0.0001	0.0580	34.73	-17	275	0.0010	0.0472	47.48
	L=5, d_i = 0.1 ± 48.6									
t	g_0	g_1	ρ	S/M	RMSE					
0.0	-152	373	-0.0051	0.0587	59.06					
0.5	-82	334	-0.0031	0.0581	58.55					
1.0	-68	313	-0.0015	0.0534	58.32					
1.5	-52	298	0.0001	0.0506	58.16					
2.0	-36	284	0.0001	0.0482	58.17					
3.0	-10	263	0.0025	0.0450	58.46					

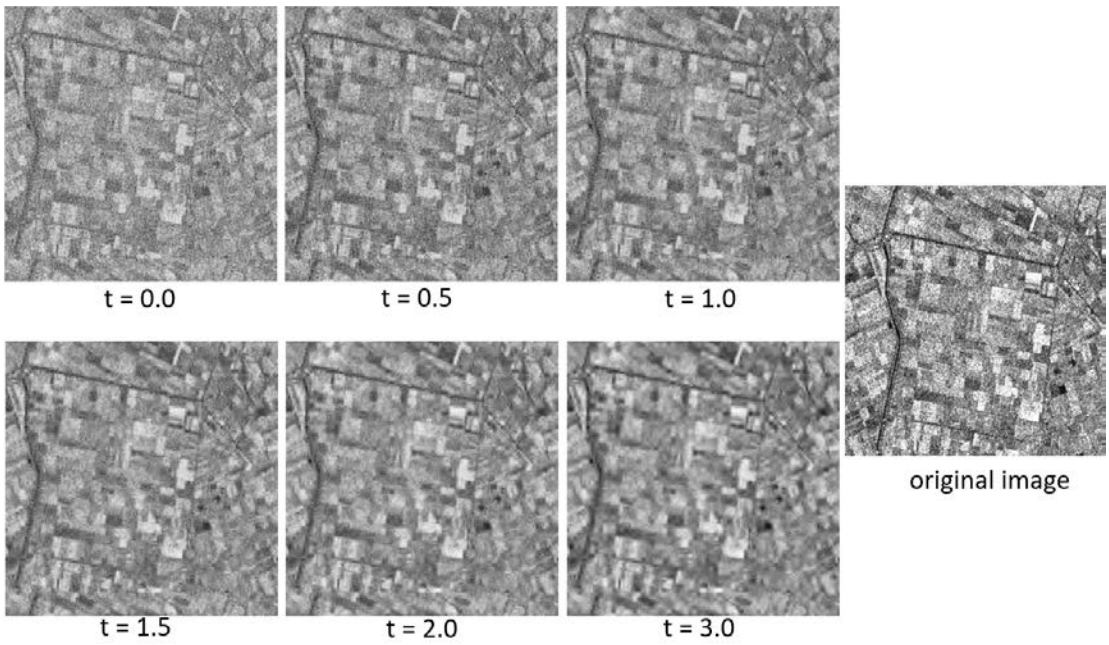

Figure 11: Soft Thresholding, L=3, A. Daub. Wavelets (N=4)

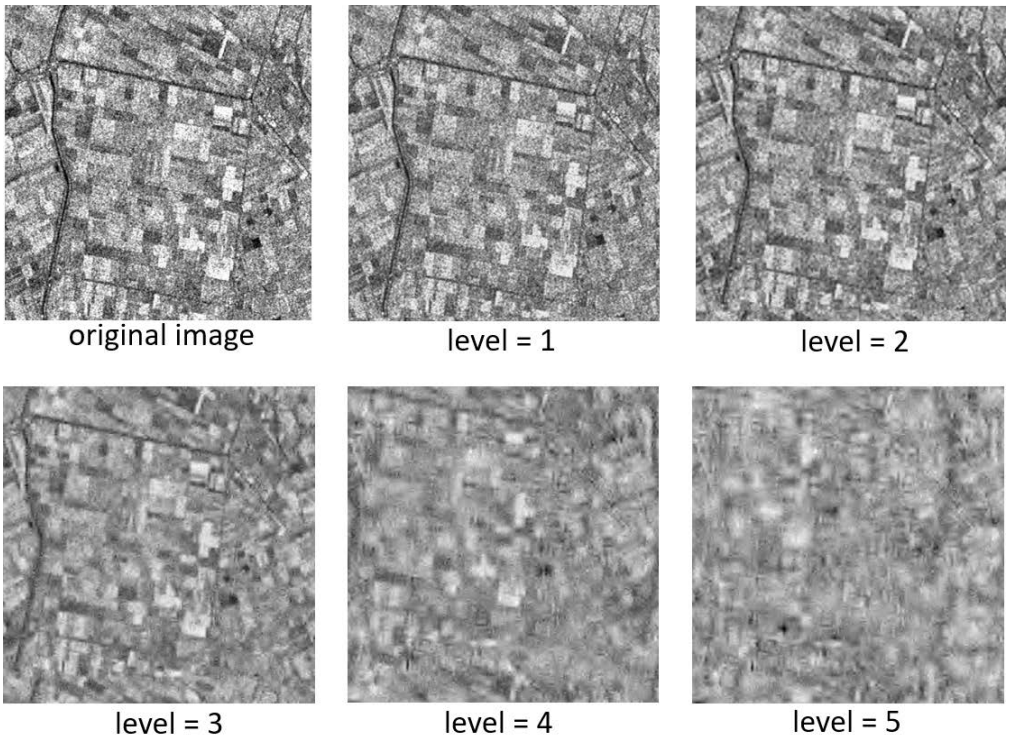

Figure 12: Soft Thresholding, A. Daub. Wavelets (N=4), t=2.0

Conclusion

1. Cross-like patterns caused by the Goldstein filter do not appear anymore in the denoised image by the method combining the multi-resolution orthogonal wavelet decomposition and reconstruction as well as the soft thresholding scheme.
2. Haar wavelets perform a better edge preservation ability with a larger ρ-values ranging from 0.0532 to 1.0000, but worse noise filtering ability with S/M-values ranging from 0.0332 to 0.2545, where the original image has the S/M-value of 0.2507.
3. The results of all 90 tests show that L=3 and t=1.5 or 2.0 will give better-denoised images for the three kinds of wavelets used in this paper, namely Haar wavelets, asymmetric Daubechies wavelets and least-asymmetric Daubechies wavelets.
4. The asymmetric Daubechies wavelets perform a worse edge preservation ability with the ρ-values ranging from -0.0059 to 0.0012, but a better performance of speckle filtering with the S/M-values ranging from 0.0450 to 0.1356, where the original image has the S/M-value of 0.2507.
5. The least-asymmetric Daubechies wavelets also perform a worse edge preservation ability with the ρ-values ranging from -0.0051 to 0.0023, but a better performance of speckle filtering with the S/M-values ranging from 0.0410 to 0.1259, where the original image has the S/M-value of 0.2507.
6. One gets a better edge preservation at the expense of a worse noise-filtering effect.
7. A larger number of levels gives a better noise-filtering effect at the expense of worse

edge preservation effect.

Recommendation

1. To fully exploit the detail components for reducing the SAR speckle, the *wavelet packets* might be adopted instead of the orthogonal wavelet analysis used in this paper.
2. The asymmetry property of Daubechies wavelets causes the image translation effect. Although it does not influence image feature interpretation at all, accurate georeferencing must be conducted using additional amendments.

Acknowledgement

We sincerely appreciate the National Science and Technology Council (NSTC), Taiwan, for the financial support to our research project for one year with the research grants NSTC 112-2121-M-006-010.

References

[1] Salepci, N., Eckardt, R. and Richter, N., (2018). Speckle filtering – Basics, Concepts & Techniques. Friedrich-Schiller University Jane, Department for Earth Observation, Jena, Germany. Retrieved in March, 2018.

[2] Fielding, E., (2024). Introduction to SAR Interferometry. Applied Remote Sensing Training (ARSET) at National Aeronautics and Space Administration(NASA). Retrieved August 15, 2024, from https://www.youtube.com/watch?v=9T1lBnta9P0.

[3] Lillesand, T.M., Kiefer, R.W., and Chipman, J.W., (2008). Remote Sensing and Image Interpretation. John Wiley & Sons, Inc., 6th edition, ISBN978-0-470-05245-7.

[4] Goldstein, R.M., & Werner, C.L., (1998), Radar interferogram filtering for geophysical applications. Geophysical Research Letters, vol. 25, No. 21, pages 4035-4038, November 1, 1998.

[5] Wu, Y.Y., and Ren, H., (2022). Discussion on Parameters of Goldstein Filtering Function of the SNAP Software. Journal of Photogrammetry and Remote Sensing (CSPRS), Vol. 27, No.4, December 2022.

[6] Tsay, J.R., (1996), Wavelets fuer das Facetten-Stereosehen. Deutsche Geodaetische Kommission, Reihe C, Heft Nr. 454, ISBN 3-7696-9497-X.

[7] Daubechies, I., (1992), Ten Lectures on Wavelets. Society for Industrial and Applied Mathematics (SIAM), ISBN: 978-0-89871-274-2.

[8] Selesnik, I., (2018), A Derivation of the Soft-Thresholding Function, Polytechnic Institute of New York University. Retrieved August 26, 2024, from chrome-extension://efaidnbmnnnibpcajpcglclefindmkaj/https://eeweb.engineering.nyu.edu/iselesni/lecture_notes/SoftThresholding.pdf

[9] Press W.H., Teukolsky S.A., Vetterling W.T., Flannery B.P., (1992). Numerical Recipes. 'Wavelet Transform'. Cambridge University Press, pp.584-599.

[10] Sattar, F., Floreby, L., Salomonsson, G., and Loevstroem, B., (1997). Image enhancement based on a nonlinear multiscale method. IEEE Transaction on Image Processing, vol. 6, No. 6, pp.888-895, June 1997.

[11] Wolf, P.R., Dewitt, B.A., and Wilkinson, B.E.,(2014), Elements of Photogrammetry with Applications in GIS, McGraw Hill Education, 4th edition, ISBN 978-9-81-460737-7.

[12] Achim, A., Tsakalides, P., and Bezerianos, A., (2003), SAR Image Denoising via Bayesian Wavelet Shrinkage Based on Heavy-Tailed Modeling, IEEE Transactions on Geoscience and Remote Sensing, vol. 41, No. 8, pp. 1773-17847, August 2003.

[13] Eineder, M., and Bamler, R., 2018. Module 1301: SAR Imaging. SAR EDU Remote Sensing Education Initiative, Remote Sensing Technology (TUM/DLR). Retrieved in March, 2018.